Applied Thermal Engineering 116 (2017) 724–730

Contents lists available at ScienceDirect

Applied Thermal Engineering

journal homepage: www.elsevier.com/locate/apthermeng

Research Paper

Diffusion of gas molecules on multilayer graphene surfaces: Dependence on the number of graphene layers

Chengzhen Sun, Bofeng Bai *

State Key Laboratory of Multiphase Flow in Power Engineering, Xi'an Jiaotong University, China

HIGHLIGHTS

- Diffusion coefficients on multilayer graphene surface are calculated.
- Gas diffusion on multilayer graphene surface is controlled by molecular collisions.
- Diffusion coefficient decrease gradually with increasing layer-number.
- Probability distribution of jump length confirms the variations of diffusion coefficient.

ARTICLE INFO

Article history:
Received 31 October 2016
Accepted 2 February 2017
Available online 5 February 2017

Keywords:
Mass transport
Surface diffusion
Multilayer graphene
Molecular dynamics

ABSTRACT

The diffusion of gas molecules on multilayer graphene surfaces is of great importance for a wide range of applications in gas-related industries. This study calculates diffusion coefficients for gas diffusion on single layer or multilayer graphene surfaces based on molecular dynamics simulations with a major emphasis on the effect of the number of graphene layers. The results show that the gas diffusion on these graphene surfaces is mainly controlled by molecular collisions in the adsorption layer; because the contributions of the gas adsorption energy and the gas collision energy are always comparable with the gas adsorption energy becoming slightly stronger with increasing number of graphene layers. Therefore, the surface diffusion coefficient decreases gradually with increasing number of graphene layers owing to the larger number of adsorbed molecules on graphene surfaces with more layers. Notably, the diffusion coefficients do not depend strongly on the number of graphene layers when there are a large number of graphene layers due to the limited interaction distance between the gas molecules and the graphene atoms. Furthermore, the variations of the surface diffusion coefficient with the number of graphene layers and the gas species are confirmed from the probability distributions of the molecular jump length on the graphene surface in a given time period.

1. Introduction

Graphene [1,2], as a representative two-dimensional material, has many applications in chemical engineering, thermal engineering and other fields [3–6]. Gas-related applications are especially important, such as graphene-based gas separation membranes [7–9], graphene-based gas sensors [10,11], thermal chemical-vapor-deposition processes for graphene production [12], and the thermal treatment of graphene oxide films in air [13,14]. In these applications, the gas diffusion characteristics on the graphene surface are very important. For example, the gas diffusion on the graphene surface restricts the permeation abilities of graphene-based membranes [15,16] and the surface diffusion characteristics determine the sensitivities of graphene-based gas sensors [10].

The surface diffusion rates reflect the mass transport characteristics on a solid surface, with the diffusion related to the molecular adsorption ability, molecular kinetic parameters and molecular collision energy [17–19]. The surface diffusion phenomena occur along the molecular adsorption layer on the solid surface where the characteristic height is on the order of nanometers. Thus, the gas diffusion phenomenon on a solid surface must be investigated at the molecular level. The relative contributions of the molecular adsorption energy and the molecular collision energy determine the surface diffusion patterns. If the molecular adsorption energy is far greater than the molecular collision energy, the surface diffusion can be described by the hopping mechanism [20–23]; otherwise, the surface diffusion would be governed by the gas behavior and would be mainly controlled by the collisions among

* Corresponding author.
E-mail address: bfbai@mail.xjtu.edu.cn (B. Bai).

http://dx.doi.org/10.1016/j.applthermaleng.2017.02.002
1359-4311/

Nomenclature

C	electrostatic constant (N m^2 C^{-2})
d	molecular kinetic diameter (m)
D	diffusion coefficient (m^2/s)
E_r	bond stretch energy (J)
E_θ	angle deformation energy (J)
K_r	bond stretch parameter (J m^{-2})
K_θ	angle deformation parameter (J rad^{-2})
M	molecular mass (kg)
P	pressure (Pa)
q_i, q_j	charges on atoms i and j (e)
r_0	equilibrium bond length (m)
t	time (s)
t_0	initial time (s)
Δt	time interval (s)
x, y	x and y coordinates of a molecule (m)
x_0, y_0	x and y coordinate at the initial time (m)

Greek symbols

ε	energy parameter (J)
σ	length parameter (m)
χ	dielectric constant (F m^{-1})
θ_0	equilibrium bond angle (rad)

adsorbed gas molecules. For graphene, the gas adsorption energy is comparable with the gas collision energy owing to the graphene being several atoms thick. Sun and Bai [24] demonstrated that gas diffusion on graphene surfaces has a gas-like behavior, mainly controlled by molecular collisions. The variation of the surface diffusion coefficient as a function of the molecular concentration is similar to that for the bulk diffusion, but the surface diffusion coefficients are lower than the bulk diffusion coefficients due to the restrictions of the molecular motion on the graphene film.

Gas-related graphene applications always involve multilayer graphene. For example, multilayer graphene is used in gas separation membranes to eliminate the effects of defects in the graphene films [8,25]. For multilayer graphene, the interactions between the graphene atoms and the gas molecules then depend on the number of graphene layers which affects the number of interacting carbon atoms. Therefore, the gas adsorption on multilayer graphene surfaces changes with the number of graphene layers and the surface diffusion characteristics then vary depending on the molecular number density on the graphene surface. These nanoscale transport phenomena are normally analyzed using molecular dynamics (MD) simulations which can accurately capture the movements of atomic particles to investigate the transport characteristics on the molecular level [26–30]. In this paper, we dedicate to study the gas diffusion characteristics on multilayer graphene surfaces by statistically calculating the surface diffusion coefficients using the Einstein equation. The surface diffusion coefficients are calculated for gaseous CH_4, H_2S, CO_2 and N_2 molecules for monolayer graphene and multilayer graphene with up to four layers. The results show the dependence of the diffusion coefficients on the number of graphene layers and the underlying mechanisms. These results have significant implications to a broad community investigating graphene materials in gas-related industries.

2. Simulation method

The MD simulations modeled a cubic box with 50 gas molecules on top of a 3×3 nm^2 multilayer graphene surface, as shown in Fig. 1(a). The simulation box height was related to the system pressure. The initial system pressure was set to 25 bar with the box height then based on the ideal gas equation for each gas set to approximately 9 nm. The simulation box height was sufficient for efficient simulations of the molecular motions on the graphene surface and avoiding the computational costs of extensive simulations of the molecular motions in the gas phase. Periodic boundary conditions were applied in the x and y directions with reflective boundary conditions in the z direction. The graphene carbon atoms were fixed during the simulations. The simulations used the NVT ensemble with a small time step of 0.134 fs, so that the system temperature equilibrated at 300 K with small fluctuations. Fig. 1 (b) and (c) display snapshots of the multilayer graphene and atomic models of the gas molecules (CH_4, H_2S, CO_2 and N_2).

The simulations modeled the CH_4 atomic interactions using the popular AIREBO potential model [31], which can be used to accurately model both chemical reactions and intermolecular interactions in hydrocarbon systems. Comparisons also show small differences between the results obtained using the AIREBO potential model and the Lennard-Jones (L-J) potential model. The other interactions were modeled using the L-J potential model coupled with Coulomb interactions:

$$\phi(r_{ij}) = \begin{cases} 4\varepsilon\left[\left(\frac{\sigma}{r_{ij}}\right)^{12} - \left(\frac{\sigma}{r_{ij}}\right)^{6}\right] + \frac{Cq_iq_j}{\chi r_{ij}} & (r_{ij} < r_{cut}) \\ 0 & (r_{ij} \geqslant r_{cut}) \end{cases} \quad (1)$$

where q_i and q_j are the charges on atoms i and j, σ is the length parameter, ε is the energy parameter, χ is the dielectric constant, and C is the electrostatic constant. The relative dielectric constants for all the gases were set to 1 with the normal values listed in Table 1 used for the L-J potential parameters and the atomic charges. The parameters ε and σ for crossing atoms were estimated by the Lorentz-Berthelot mixing rule. The cutoff distances for the van der Waals interactions and the short-range Columbic interactions were both set to 10 Å. The bond stretch energy, E_r, and the bond angle deformation energy, E_θ, within a gas molecule were defined based on the Harmonic model as:

$$\begin{aligned} E_r &= K_r(r - r_0)^2 \\ E_\theta &= K_\theta(\theta - \theta_0)^2 \end{aligned} \quad (2)$$

where r_0 is the equilibrium bond length, θ_0 is the equilibrium bond angle, K_r is the bond stretch parameter, and K_θ is the angle deformation parameter. These parameters for H_2S, CO_2 and N_2 are listed in Table 2. The bond information in CH_4 molecules is already included in the AIREBO potential model.

The surface diffusion occurs in the molecular adsorption layer on the graphene surface. The Einstein equation was used to calculate the statistics for the gas diffusion coefficients on the graphene surface based on the coordinates of the molecules moving in the adsorption layer. The Einstein equation is:

$$D = \frac{\langle (x - x_0)^2 + (y - y_0)^2 \rangle}{4\Delta t} \quad (3)$$

where D is the gas diffusion coefficient (m^2/s), x and y are the x and y coordinates of the molecule at time, t, x_0 and y_0 are the x and y coordinates at time t_0 (the initial time for the molecules entering the adsorption layer), and Δt equals t–t_0. The model for calculating the diffusion coefficient on multilayer graphene surface is illus-

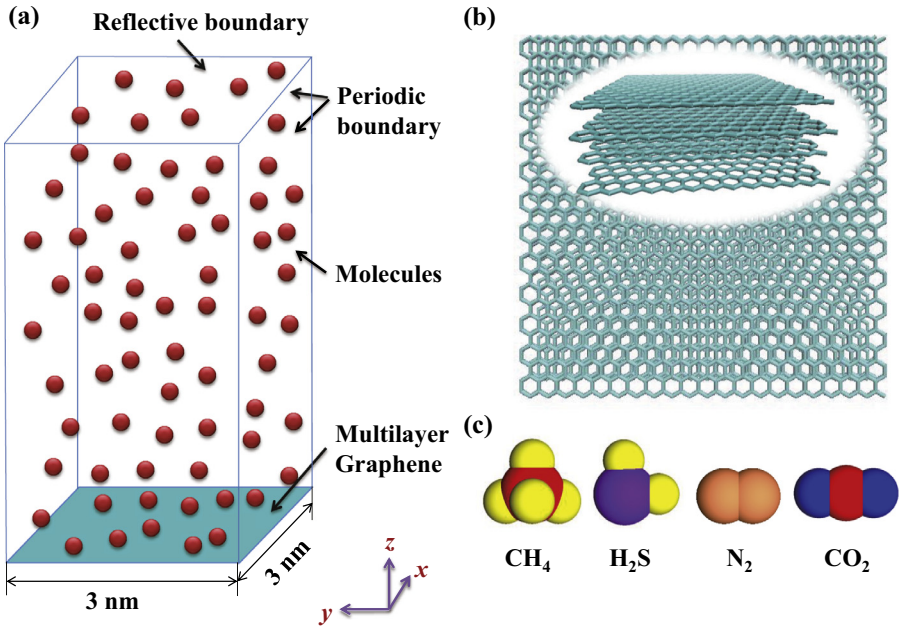

Fig. 1. Simulation system for gas diffusion on multilayer graphene surface. (a) Simulation box; (b) Snapshot of multilayer graphene; (c) Atomic models of gas molecules.

Table 1
L-J potential parameters and atomic charges used in the simulation.

	ε/eV	σ/Å	Charge/e
Graphene [27]			
C—C	2.413×10^{-3}	3.400	/
H_2S [32]			
H—H	0.336×10^{-3}	0.98	0.124
H—S	2.691×10^{-3}	2.35	/
S—S	21.545×10^{-3}	3.72	−0.248
CO_2 [33]			
C—C	2.424×10^{-3}	2.757	0.6512
C—O	4.101×10^{-3}	2.895	/
O—O	6.938×10^{-3}	3.033	−0.3256
N_2 [34]			
N—N	3.126×10^{-3}	3.297	0

Table 2
Bond and angle Harmonic potential parameters for the gas molecules.

	E_r	
	K_r/eV Å^{-2}	r_0/Å
H—S (H_2S) [35]	2.021	1.365
C—O (CO_2) [35]	6.158	1.160
N—N (N_2) [36]	1.426	1.112
	E_0	
	K_0/eV rad^{-2}	θ_0/°
H—S—H (H_2S) [37]	1.110	91.5
O—C—O (CO_2) [38]	6.416	180

trated in Fig. 2. Actually, the diffusion coefficient was calculated based on the linear relationship between the mean-square displacement in the x-y plane $\left(\langle (x-x_0)^2 + (y-y_0)^2 \rangle\right)$ and the time interval, Δt, of the gas molecules moving in the adsorption layer on the graphene surface. The simulations started with an equilibrium run with 50 million time steps followed by 2 million time steps with a data recording period of 250 time steps to calculate the diffusion coefficient. The 2 million time steps ensured a large sample set for the molecular diffusion on the graphene surface while the data recording period of 250 time steps gave a high resolution snapshot of the gas molecule trajectories on the graphene surface.

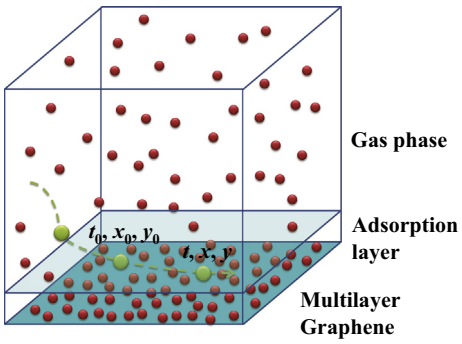

Fig. 2. Model for calculating diffusion coefficients on multilayer graphene surface.

3. Results and discussion

3.1. Adsorption layer

The molecular adsorption characteristics on the multilayer graphene surface were investigated first because the gas adsorption characteristics significantly impact the surface diffusion. Owing to the strong interactions between the gas molecules and the graphene atoms near the surface, the gas molecules can adsorb onto the graphene surface to form a high-density zone, as seen from Fig. 3(a) which shows the molecular density distribution along the z-direction for CH_4 molecules adsorbed onto the monolayer graphene surface. The high-density zone and the bulk zone are both indicated at $z = 0.6$ nm. The high-density zone (denoted as the adsorption layer) exhibits an atomic thickness, indicating that only one layer of gas molecules can adsorb onto the graphene surface. Fig. 3(b) shows the number of adsorbed molecules on the multilayer graphene surface versus the number of graphene layers for different gas molecules. The gas adsorption intensity depends on the number of graphene layers with more layers of graphene leading to higher adsorption intensities. This is related to the

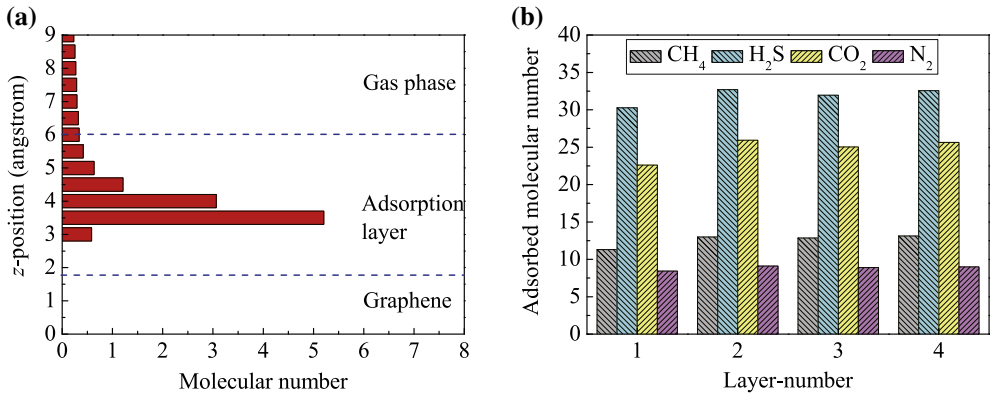

Fig. 3. Molecular adsorption characteristics on multilayer graphene surface. (a) Molecular number density distribution along *z*-direction for CH_4 adsorbed on surface of monolayer graphene. (b) Number of adsorbed gas molecules on the multilayer graphene surface with different number of graphene layers.

increase in the number of carbon atoms in the multilayer graphene that interact with the adsorbed molecules which strengthens the interactions between the gas molecules and the graphene and then the adsorption of the gas molecules. However, the adsorption intensities for the two-, three- and four-layer graphene samples are very similar due to the limited effective interaction distances between the gas molecules and the graphene atoms. Although there are more carbon atoms in the multilayer graphene, the number of effective carbon atoms which can interact with the gas molecules varies very little as the number of graphene layers increases past 2. Therefore, the adsorption intensities have a weak dependence on the number of graphene layers for more than 2 layers. For the same number of graphene layers, the adsorption intensities for different gas species differ due to their distinct atomic interactions with the adsorption intensities increasing from N_2 to CH_4 to CO_2 to H_2S.

3.2. Diffusion coefficient

The surface diffusion coefficients were calculated based on the Einstein equation. In this calculation, the linear relationship between the mean-square displacement in the *x-y* plane versus the time interval for gas molecules diffusing on the multilayer graphene surface is very crucial. Fig. 4 shows an example of the mean-square displacement versus the time interval for CH_4 molecules diffusing on the surface of monolayer graphene. As seen from the figure, the line has different patterns in different parts with the left-part of the line exhibiting poor linearity, the right-part of the line being discontinuous, and only the central-part having good

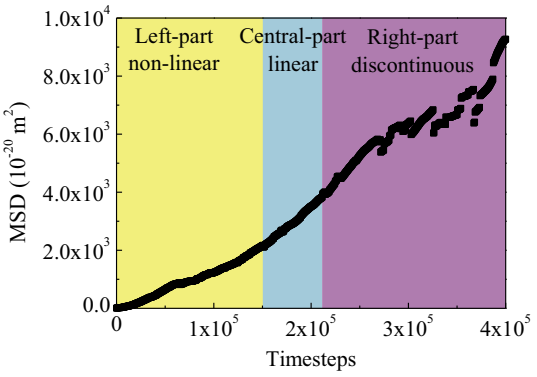

Fig. 4. Mean-square displacement in *x-y* plane versus time interval for CH_4 molecules diffusing on monolayer graphene surface.

linearity, so only the central part can be used to calculate the diffusion coefficients. Along the left part of the line, many of the partially adsorbed molecules may quickly move out the adsorption layer with little diffusion on the graphene surface; consequently, the mean-square displacement is not linearly related to the time interval. For the right part of the line, few of the adsorbed molecules have diffused on the graphene surface for relatively long time periods so mean-square displacement line is not continuous. The surface diffusion coefficient can then only be obtained by fitting the slope of the central part of the line. The boundaries of the central part of the line should then be carefully determined to ensure that the calculation of the diffusion coefficient has a small uncertainty. The slope of the central part of the line will differ for multilayer graphene with different numbers of graphene layers, resulting in a dependence of the diffusion coefficients on the number of graphene layers.

Sun and Bai [24] showed that gas diffusion on monolayer graphene surfaces has two-dimensional gas-like behavior because the gas adsorption energy is comparable to the gas collision energy. Although the gas adsorption energy strengthens slightly with increasing number of graphene layers, the relative contributions of the gas adsorption energy and the gas collision energy remain the same; thus, the gas diffusion on the multilayer graphene surface is always mainly controlled by the collisions among the adsorbed molecules. Therefore, the gas diffusion on the multilayer graphene surface is similar to bulk diffusion, regardless of the number of graphene layers. This conclusion can be seen in the regular probability distribution of the molecular jump length on the graphene surface as discussed in the next section. For the multilayer graphene, the diffusion coefficient decreases gradually with increasing number of graphene layers, as seen in Fig. 5. An increasing number of graphene layers increases the number density of the adsorbed molecules as seen in Fig. 3 due to the increasing number of interacting graphene atoms. Thus, for the multilayer graphene with more layers, more molecules are concentrated on the graphene surface and the diffusive movements of the gas molecules are more restricted through collisions with adjacent molecules. Consequently, the surface diffusion coefficient decreases with more graphene layers for the same gas species. The effect of the number of graphene layers on the diffusion coefficient then rapidly weakens as the number of graphene layers increases to a large value because there is less increase in the molecular adsorption intensity with a larger number of layers.

The diffusion coefficients differ for different gas species with the same number of graphene layers due to the distinctive molecular kinetic parameters for each gas species as also seen in Fig. 5. Due to the gas-like behavior, the gas diffusion on the graphene sur-

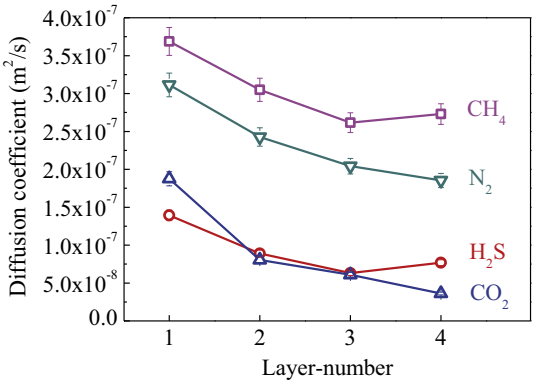

Fig. 5. Variations of diffusion coefficient versus number of graphene layers for CH_4, H_2S, CO_2 and N_2, respectively. The error bars of diffusion coefficients are plotted based on an uncertainty of 5%.

face can be explained by the hard sphere model for ideal gases where the diffusion coefficients, D, are inversely proportion to the square root of the molecular mass ($M^{1/2}$) and the square of the kinetic diameter (d^2). The CH_4 (d = 0.38 nm, M = 16.04) and N_2 (d = 0.364 nm, M = 28.01) molecules have small masses, resulting in high diffusion coefficients. Compared with the CO_2 (d = 0.33 nm, M = 44.01) molecules, the H_2S (d = 0.36 nm, M = 34.08) molecules have smaller masses but larger diameters, resulting in comparable diffusion coefficients for CO_2 and H_2S molecules. The strong adsorption capabilities of CO_2 and H_2S molecules further weaken their diffusion rates as more molecules concentrate on the graphene surface. The pressures in the gas phase differ for different gas species and different numbers of graphene layers. The pressure of the gas phase is lower for the gas species with stronger adsorption intensities, because more molecules are adsorbed on the graphene surface so there are fewer molecules in the gas phase. If the gas phase pressure were the same in all the simulations, the dependence of the diffusion coefficient on the number of graphene layers would be more obvious, because more molecules would be adsorbed onto the multilayer graphene surface with more layers.

3.3. Molecular jump length

The probability distribution of the molecular jump length on the graphene surface further confirms the variations of the surface diffusion coefficient with the number of graphene layers and gas species. The molecular jump length on the graphene surface was obtained using a 250 time step time period. Fig. 6 shows the probability distributions of the molecular jump length on the multilayer graphene surface for various numbers of graphene layers for CH_4, H_2S, CO_2 and N_2 molecules. The probability distributions are presented as regular distributions, *i.e.* low probabilities for small and large jump lengths and high probabilities for the moderate jump lengths. These distribution characteristics demonstrate that the gas diffusion on the graphene surface is similar to diffusion in a gas controlled by molecular collisions because only gas-like diffusion can produce the regular probability distributions of the molecular jump length with zero-probability of zero-jump length and arbitrary values of jump length over some range. A higher average jump length means a faster molecular diffusion rate on the graphene surface. With the regular probability distribution of the molecular jump length, a wider distribution and a higher maximum probability jump length generally produces a higher average jump length. The variations of the probability distribution profiles with the gas species in Fig. 6 are basically consistent with those of the diffusion coefficient. For example, the CH_4 and N_2 molecules have wider probability distributions than those of the H_2S and CO_2 molecules, consistent with the higher diffusion coefficients of the CH_4 and N_2 molecules. However, the probability distribution profiles have a weak dependence on the number of graphene layers, meaning that the average molecular velocity is independent of the number of graphene layers. The hard sphere model for gas diffusion indicates that the lower diffusion coefficient on multilayer graphene with more layers is caused by the shorter mean free paths of the molecular motion due to more molecules on the graphene surface.

The differences in the number of samples having a particular jump length for the different gas species and the different numbers of graphene layers is related to the different molecular adsorption intensities on the graphene surface of the various species, with higher molecular adsorption intensities leading to more molecules diffusing on the graphene surface. The number of samples for a particular jump length is consistent with the molecular adsorption intensity which decreases from H_2S to CO_2 to CH_4 to N_2. However, a higher number of samples does not necessarily mean that more molecules enter into the adsorption layer, but indicates that the adsorbed molecules stay in the adsorption layer for a longer time period. Fig. 7 shows the total number of molecules entering the adsorption layer during the 2 million time step run, but this number does not account for how long time the adsorbed molecule stays in the adsorption layer. This data shows that the total number of molecules does not change much with the number of graphene layers or the gas species because this number is related to the gas phase pressure and the molecular mass as given by kinetic theory of ideal gas. Fig. 7 also shows the number of molecules versus the number of time steps that the molecules stay in the adsorption layer during the 2 million time steps for CH_4 diffusing on a monolayer surface. The total number of molecules shown in the insert is just the maximum of the number of molecules at the left end of the curve. The curve descends very sharply initially since many of the partially adsorbed molecules quickly return to the gas phase. This phenomenon is consistent with the non-linear left part of the line for the mean-square displacement versus time shown in Fig. 4.

4. Conclusions

Diffusion coefficients were calculated for four gas molecules (CH_4, H_2S, CO_2 and N_2) on single or multilayer graphene surfaces (monolayer to four layers) based on MD simulations to show the dependence of surface diffusion coefficients on the number of graphene layers. The diffusion coefficients were calculated using the Einstein equation based on the trajectories of the molecules moving on the graphene surface. The results show that gas diffusion on multilayer graphene surfaces has a gas-like behavior that is mainly controlled by the molecular collisions, because the gas adsorption energy is always comparable with the gas collision energy and their relative contributions remain the same for different numbers of graphene layers. As the number of graphene layers increases, the diffusive movements of the gas molecules on the graphene surface slow due to the presence of more molecules on the graphene surface, so the surface diffusion coefficient gradually decreases. The diffusion coefficient is only weakly dependent on the number of graphene layers with a large number of graphene layers because the molecular number density on the graphene surface is only weakly related to the number of graphene layers due to the limited gas-graphene interaction distance. For the same number of graphene layers, the diffusion coefficients of the various gas species differ due to their different molecular diameters and masses. The dependence of the surface diffusion coefficient on the number of graphene layers and the gas species is further confirmed by the

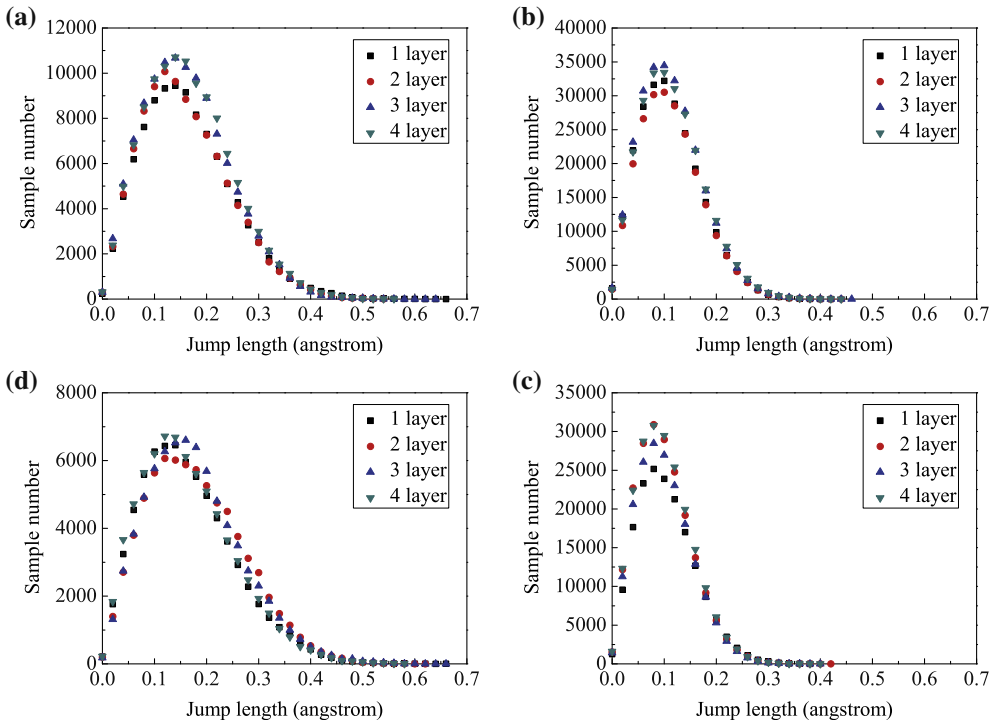

Fig. 6. Probability distribution of molecular jump length in a certain time period on multilayer graphene surface with different number of graphene layers. (a) CH_4, (b) H_2S, (c) CO_2 and (d) N_2.

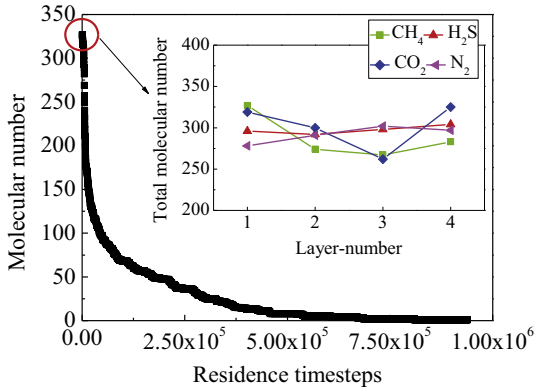

Fig. 7. Variation of the total number of molecules entering into the adsorption layer in the run of 2 million time steps.

probability distribution of the molecular jump length on the graphene surface for a given time period. These results provide a theoretical guide for the application of multilayer graphene in gas-related industries and provide new insights into surface diffusion phenomena. Further attention should be paid to the effects of chemical functionalization of the graphene surface and others effects such as graphene defects and physical fluctuations.

Acknowledgments

Financial support from the NSFC for Distinguished Young Scientists (No. 51425603) and general program (No. 51506166) and the Project Funded by the China Postdoctoral Science Foundation (No. 2015M580846) are greatly appreciated.

References

[1] A.K. Geim, K.S. Novoselov, The rise of graphene, Nat. Mater. 6 (2007) 183–191.
[2] A.K. Geim, Graphene: status and prospects, Science 324 (2009) 1530–1534.
[3] Z. Shomali, A. Abbassi, J. Ghazanfarian, Development of non-Fourier thermal attitude for three-dimensional and graphene-based MOS devices, Appl. Therm. Eng. 104 (2016) 616–627.
[4] Y. Sun, B. Tang, W. Huang, S. Wang, Z. Wang, X. Wang, Y. Zhu, C. Tao, Preparation of graphene modified epoxy resin with high thermal conductivity by optimizing the morphology of filler, Appl. Therm. Eng. 103 (2016) 892–900.
[5] C. Sun, B. Wen, B. Bai, Recent advances in nanoporous graphene membrane for gas separation and water purification, Sci. Bull. 60 (2015) 1807–1823.
[6] C. Sun, B. Wen, B. Bai, Application of nanoporous graphene membranes in natural gas processing: molecular simulations of CH_4/CO_2, CH_4/H_2S and CH_4/N_2 separation, Chem. Eng. Sci. 138 (2015) 616–621.
[7] K. Celebi, J. Buchheim, R.M. Wyss, A. Droudian, P. Gasser, I. Shorubalko, J.-I. Kye, C. Lee, H.G. Park, Ultimate permeation across atomically thin porous graphene, Science 344 (2014) 289–292.
[8] H.W. Kim, H.W. Yoon, S.-M. Yoon, B.M. Yoo, B.K. Ahn, Y.H. Cho, H.J. Shin, H. Yang, U. Paik, S. Kwon, J.-Y. Choi, H.B. Park, Selective gas transport through few-layered graphene and graphene oxide membranes, Science 342 (2013) 91–95.
[9] G. Liu, W. Jin, N. Xu, Graphene-based membranes, Chem. Soc. Rev. 44 (2015) 5016–5030.
[10] R.K. Paul, S. Badhulika, N.M. Saucedo, A. Mulchandani, Graphene nanomesh as highly sensitive chemiresistor gas sensor, Anal. Chem. 84 (2012) 8171–8178.
[11] S.S. Varghese, S. Lonkar, K.K. Singh, S. Swaminathan, A. Abdala, Recent advances in graphene based gas sensors, Sens. Actuat. B – Chem. 218 (2015) 160–183.
[12] K. Yan, L. Fu, H. Peng, Z. Liu, Designed CVD growth of graphene via process engineering, Acc. Chem. Res. 46 (2013) 2263–2274.
[13] E. Tegou, G. Pseiropoulos, M.K. Filippidou, S. Chatzandroulis, Low-temperature thermal reduction of graphene oxide films in ambient atmosphere: infra-red spectroscopic studies and gas sensing applications, Microelectron. Eng. 159 (2016) 146–150.
[14] Q. Pan, C.-C. Chung, N. He, J.L. Jones, W. Gao, Accelerated thermal decomposition of graphene oxide films in air via in situ X-ray diffraction analysis, J. Phys. Chem. C 120 (2016) 14984–14990.
[15] L.W. Drahushuk, M.S. Strano, Mechanisms of gas permeation through single layer graphene membranes, Langmuir 28 (2012) 16671–16678.
[16] C. Sun, M.S.H. Boutilier, H. Au, P. Poesio, B. Bai, R. Karnik, N.G. Hadjiconstantinou, Mechanisms of molecular permeation through nanoporous graphene membranes, Langmuir 30 (2014) 675–682.
[17] E. Garcia-Perez, P. Serra-Crespo, S. Hamad, F. Kapteijn, J. Gascon, Molecular simulation of gas adsorption and diffusion in a breathing MOF using a rigid force field, Phys. Chem. Chem. Phys. 16 (2014) 16060–16066.

[18] N.E.R. Zimmermann, B. Smit, F.J. Keil, Predicting local transport coefficients at solid-gas interfaces, J. Phys. Chem. C 116 (2012) 18878–18883.
[19] A. Ramirez, Anisotropic diffusion of hydrogen in nanoporous carbons, J. Mater. Sci. 49 (2014) 7087–7098.
[20] S.-T. Hwang, K. Kammermeyer, Surface diffusion in microporous media, Can. J. Chem. Eng. 44 (1966) 82–89.
[21] R.T. Yang, J.B. Fenn, G.L. Haller, Modification to the Higashi model for surface diffusion, AIChE J. 19 (1973) 1052–1053.
[22] E.R. Gilliland, R.F. Baddour, G.P. Perkinson, K.J. Sladek, Diffusion on surfaces. I. Effect of concentration on the diffusivity of physically adsorbed gases, Ind. Eng. Chem. Fund. 13 (1974) 95–100.
[23] Y.D. Chen, R.T. Yang, Concentration dependence of surface diffusion and zeolitic diffusion, AIChE J. 37 (1991) 1579–1582.
[24] C. Sun, B. Bai, Gas diffusion on graphene surfaces, Phys. Chem. Chem. Phys. 19 (2017) 3894–3902.
[25] M.S.H. Boutilier, C. Sun, S.C. O'Hern, H. Au, N.G. Hadjiconstantinou, R. Karnik, Implications of permeation through intrinsic defects in graphene on the design of defect-tolerant membranes for gas separation, ACS Nano 8 (2014) 841–849.
[26] C.-Z. Sun, W.-Q. Lu, B.-F. Bai, J. Liu, Novel flow behaviors induced by a solid particle in nanochannels: Poiseuille and Couette, Chinese Sci. Bull. 59 (2014) 2478–2485.
[27] H.L. Du, J.Y. Li, J. Zhang, G. Su, X.Y. Li, Y.L. Zhao, Separation of hydrogen and nitrogen gases with porous graphene membrane, J. Phys. Chem. C 115 (2011) 23261–23266.
[28] T. Wu, Q. Xue, C. Ling, M. Shan, Z. Liu, Y. Tao, X. Li, Fluorine-modified porous graphene as membrane for CO_2/N_2 separation: molecular dynamic and first-principles simulations, J. Phys. Chem. C 118 (2014) 7369–7376.
[29] L. Li, J. Mo, Z. Li, Nanofluidic diode for simple fluids without moving parts, Phys. Rev. Lett. 115 (2015) 134503.
[30] B. Wen, C. Sun, B. Bai, Inhibition effect of a non-permeating component on gas permeability of nanoporous graphene membrane, Phys. Chem. Chem. Phys. 17 (2015) 23619–23626.
[31] S.J. Stuart, A.B. Tutein, J.A. Harrison, A reactive potential for hydrocarbons with intermolecular interactions, J. Chem. Phys. 112 (2000) 6472–6486.
[32] G. Lei, C. Liu, H. Xie, F. Song, Separation of the hydrogen sulfide and methane mixture by the porous graphene membrane: effect of the charges, Chem. Phys. Lett. 599 (2014) 127–132.
[33] H. Liu, S. Dai, D. Jiang, Insights into CO_2/N_2 separation through nanoporous graphene from molecular dynamics, Nanoscale 5 (2013) 9984–9987.
[34] K. Chae, A. Violi, Mutual diffusion coefficients of heptane isomers in nitrogen: a molecular dynamics study, J. Chem. Phys. 134 (2011) 044537.
[35] http://www.wiredchemist.com/chemistry/data/bond_energies_lengths.html.
[36] T.L. Cottrell, The Strengths of Chemical Bonds, Butterworths Publications Ltd., London, 1958.
[37] G. Kamath, N. Lubna, J.J. Potoff, Effect of partial charge parametrization on the fluid phase behavior of hydrogen sulfide, J. Chem. Phys. 123 (2005) 124505.
[38] J.G. Harris, K.H. Yung, Carbon dioxides liquid-vapor coexistence curve and critical properties as predicted by a simple molecular-model, J. Phys. Chem. 99 (1995) 12021–12024.